

# Evaluation of Dorim-Goh bridge using ambient trucks through short-period structural health monitoring system

Mosbeh R. Kaloop<sup>1,2,3a</sup>, Won Sup Hwang<sup>4b</sup>, Emad Elbeltagi<sup>5c</sup>, Ashraf Beshr<sup>3d</sup> and Jong Wan Hu<sup>\*1,2</sup>

<sup>1</sup>Department of Civil and Environmental Engineering, Incheon National University, Korea  
<sup>2</sup>Incheon Disaster Prevention Research Center, Incheon National University, Incheon, Korea  
<sup>3</sup>Public Works and Civil Engineering Department, Mansoura University, Egypt  
<sup>4</sup>Department of Civil Engineering, Inha University, Incheon, Korea  
<sup>5</sup>Structural Engineering Department, Mansoura University, Mansoura, Egypt

(Received August 8, 2018, Revised December 18, 2018, Accepted December 31, 2018)

**Abstract.** This paper aims to evaluate the behavior of Dorim-Goh bridge in Seoul, Korea, under static and dynamic loads effects by ambient trucks. The prestressed concrete (PSC) girders and reinforcement concrete (RC) slab of the bridge are evaluated and assessed. A short period monitoring system is designed which comprises displacement, strain and accelerometer sensors to measure the bridge performance under static and dynamic trucks loads. The statistical analysis is used to assess the static behavior of the bridge and the wavelet analysis and probabilistic using Weibull distribution are used to evaluate the frequency and reliability of the dynamic behavior of the bridge. The results show that the bridge is safe under static and dynamic loading cases. In the static evaluation, the measured neutral axis position of the girders is deviated within 5% from its theoretical position. The dynamic amplification factor of the bridge girder and slab are lower than the design value of that factor. The Weibull shape parameters are decreased, it which means that the bridge performance decreases under dynamic loads effect. The bridge girder and slab's frequencies are higher than the design values and constant under different truck speeds.

**Keywords:** monitoring; bridge; wavelet; safety; dynamic

## 1. Introduction

Many highway and railway bridges are constructed last decades in Seoul, Korea, to connect its different cities and to smooth and facilitate the transportation among these cities (Ducruet *et al.* 2012). With the absence of permanent monitoring systems to evaluate the bridges' behavior, periodic short monitoring systems are used (Kim *et al.* 2014, Kaloop *et al.* 2016). The results of these measurements are compared and reported based on design simulation models (Kim *et al.* 2014). In this study, a short monitoring system with high sampling rate of strain, displacement and accelerometer sensors measurements are used to assess Dorim-Goh bridge under the effect of design traffic loads.

On the other hand, the behavior of bridges should be evaluated experimentally or by simulating the bridges or taking real measurements from sites (Sohn *et al.* 2004, Seo

*et al.* 2016, Koto *et al.* 2019). Real observation systems reflect the exact performance of structures, consequently, this study uses this evaluation system to detect the Dorim-Goh bridge performance. The load system that used to evaluate the bridges' behavior is presented and discussed by the American Association of State Highway and Transportation Officials (AASHTO) (Sohn *et al.* 2004, Seo *et al.* 2013, Peiris and Harik 2016). Therefore, the AASHTO rules are used to design trucks loads in static and dynamic evaluation systems. Bridges deflections and stresses are measured to evaluate their static behavior, while dynamic behavior is evaluated in time and frequency domains (Sohn *et al.* 2004). Womack *et al.* (2001) assessed the deflection of steel girder bridge using real measurements based on AASHTO rules. Caglayan *et al.* (2012) evaluated the static and dynamic behavior of concrete arch bridge using simulation model. Naser and Wang (2013) evaluated a prestressed concrete (PSC) box girder using real measurements of strains. Phares *et al.* (2013) detected the damage of U.S. 30 bridge using statistical algorithm based on real measurements. Yang *et al.* (2016) used simulation to assess static and dynamic behaviors of a suspension bridge. These studies reveal that static and dynamic evaluation can be used to detect the changes in the boundary conditions of bridges and study their safety.

The boundary conditions via natural frequency is one of the parameters that should be measured and assessed (Sohn *et al.* 2004). The fast Fourier transformation (FFT) is used to extract the frequencies of structures, but the energies of

\*Corresponding author, Associate Professor

E-mail: [jongp24@inu.ac.kr](mailto:jongp24@inu.ac.kr)

<sup>a</sup>Associate Professor

E-mail: [mosbeh@mans.edu.eg](mailto:mosbeh@mans.edu.eg)

<sup>b</sup>Professor

E-mail: [hws@inha.ac.kr](mailto:hws@inha.ac.kr)

<sup>c</sup>Professor

E-mail: [eelbelta@mans.edu.eg](mailto:eelbelta@mans.edu.eg)

<sup>d</sup>Assistant Professor

E-mail: [eng.aabeshr@yahoo.com](mailto:eng.aabeshr@yahoo.com)

that frequencies should be evaluated to extract the real behavior of structures in frequency domain (Farzampour *et al.* 2018a, b). Li *et al.* (2009) used the acceleration data and wavelet analysis to assess the dynamic behavior of buildings, and they concluded that the wavelet can be used to provide a deep understanding of structures through time-frequency evaluation. Sayed *et al.* (2017) assessed a railway bridge using strain measurements and wavelet analysis, and they found that the wavelet can be used to assess the powers and energies of frequencies contents. Farzampour *et al.* (2018a, b) utilized the wavelet-transformation with independent component analysis to identify the dynamic parameters of structures, and they concluded that the developed method can be used to specify the accurate performance of structures. In addition, the wavelet analysis is used to assess and detect the damages of structures (Shahsavari 2017, Farzampour *et al.* 2018b). In this study, the wavelet analysis is used to extract the actual dynamic behavior of Dorim-Goh bridge through the acceleration measurements using wavelet energy of the wavelet decomposition levels.

In the other hand, the dynamic factor (DF) and reliability of the bridge is studied and discussed. The DF value considered the following factors to assess the capacity of bridge: bridge span length and natural frequency, the traffic volume and speed, weight and dynamic characteristics, the condition of the bridge structures-roadway roughness, expansion joint's condition and others (Paeglite and Paeglitis 2013). The DF or dynamic amplification factor have been utilized to study the dynamic capacity of bridges' girders (Hwang and Nowak 1989, Paeglite and Paeglitis 2013, Yan *et al.* 2017, Seo *et al.* 2017, Fatmi *et al.* 2018). In addition, the DF is used to evaluate the dynamic behavior of bridges through studying the effect of traffic loads positions (Paeglite and Paeglitis 2013, Huang 2001). Meanwhile, the reliability of structures is essential in the assessment of the structures feasibility, integrity and safety (Modares and Taha 2014). Also, it is considered as a rational evaluation to provide a good basis for the decision about repair, rehabilitation or replacement (Nowak and Szerszen 2000). Therefore, many researchers developed models that can be used to assess the reliability of structures. The probability model is the common used model in the design codes of many countries to analyze the reliability of structures (Nowak and Szerszen 2000, Ren and Yue 2018, Vaez and Saeid 2018, Monarrez 2018). The degree of the probability of structures failure rate refers to the degree of safety. Weibull, Log-normal, Bernoulli distribution, etc., are some distribution functions that used in the applications of reliability (Vaez and Saeid 2018). Herein, it should be mentioned that the random and non-precise probability variables may give rise to misleading results, therefore, the uncertainty of data should be studied (Liu *et al.* 2017, Zhang *et al.* 2018). Kim and Sitar (2013) used the probability theory to evaluate the soil slope stability, and they found it a significant tool to study the reliability of soil slope. In addition, the pillar stability in the mining application is evaluated using a probability model (Kim and Sitar 2013). Liu *et al.* (2018) utilized the probability model to evaluate the reliability of space steel

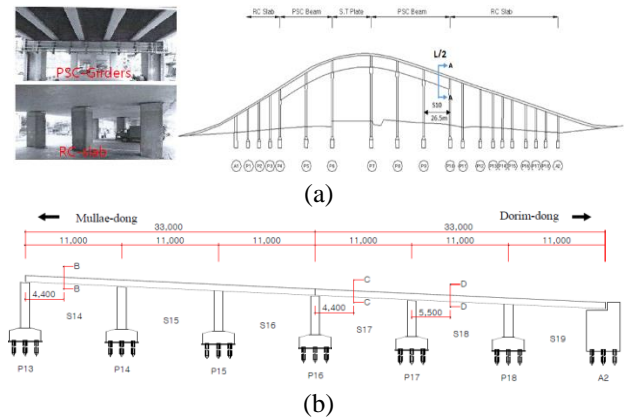


Fig. 1 Bridge and test spans overviews (a) bridge parts and PSC girder monitoring section, (b) RC slab monitoring sections

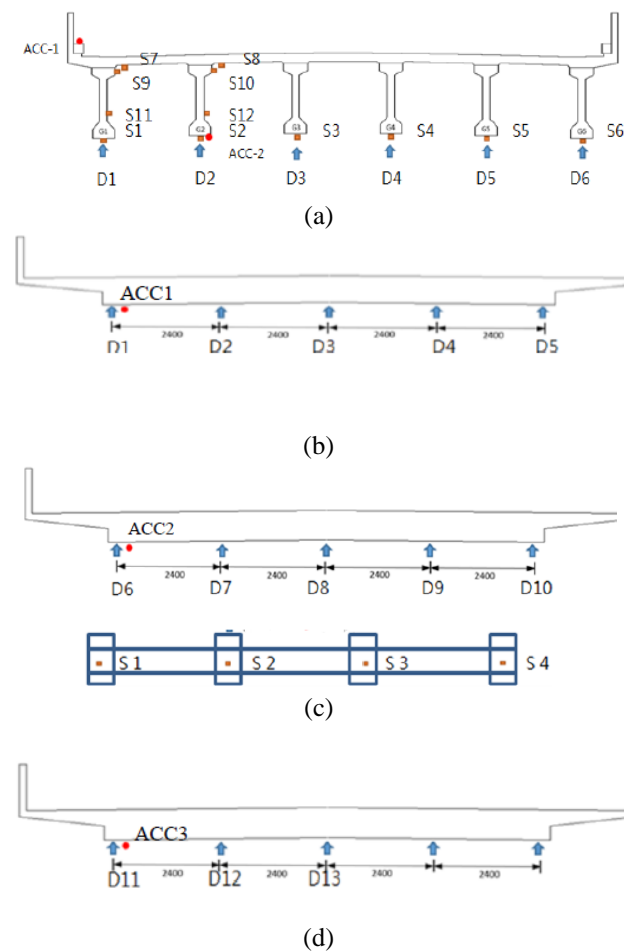


Fig. 2 Bridge cross sections and monitoring system of (a) PSC girder (section A-A), (b) RC section B-B, (c) RC section C-C, (d) RC section D-D

structures. Fan and Liu (2018), Strauss *et al.* (2009) and Wang (2010) used different probability models to assess the reliability of existing bridges.

In this study, real measurements are collected for the Dorim-Goh bridge to assess its safety. Static and dynamic loads, through using ambient trucks, are used to assess bridge's behavior in time and frequency domains. The

accurate frequencies contents of the bridge are estimated using wavelet energy analysis under different cases of loading. Moreover, the bridge DF and reliability are analyzed to assess the bridge safety.

**2. Material and methods**

*2.1 Bridge and monitoring system description*

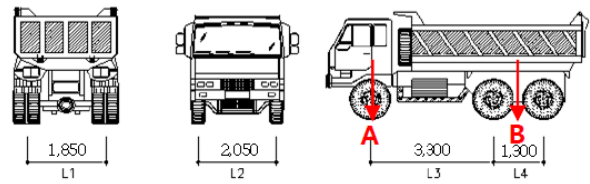
Dorim-Goh bridge is located in Seoul, Korea, and connects Dorimsa street and Mullae-dong cross-roads. The bridge is completed in 1974 and repaired in 1996. Various structural types are used to construct the bridge. As presented in Fig. 1, the reinforcement concrete (RC) is used between piers A1 to P4 and between P10 to A2, while the prestressed concrete (PSC) beam girder is used between piers P4 to P6 and between piers P7 to P10. The steel plate girder is used between piers P6 and P7. The total length of the bridge is 325.70 m and its width ranges from 9.8 m to 13.60 m.

Fig. 2 shows the cross section of the bridge. Four sections are selected to test the bridge PSC beam girder and RC slab in year 2016 (2016-test) based on the evaluation test occurred in year 1996 (1996-test). In addition, the same conditions for the load positions and trucks types of 1996-test are used in 2016-test. The monitoring system is used to assess the bridge performance under different static and dynamic loading cases to evaluate the static, semi-static and dynamic behavior of the bridge.

To analyze the performance of the PSC girder (section A-A) and the RC slab (sections B-B, C-C and D-D) of the bridge (Fig. 1), a short monitoring system is used. This evaluation is conducted based on periodic government tests for the public infrastructures to assess their performance. In this monitoring system, the strain, displacement and accelerometer sensors are used to assess the static and dynamic performance of the bridge. Table 1 shows the sensors types and the instruments used in the monitoring system of the bridge. A 200 Hz sampling frequency sensors is used. Fig. 2 shows the bridge cross sections and the monitoring system. The monitoring system of the PSC girder comprises of two accelerometer (ACC) sensors to measure the acceleration of the girder and the slab. In addition, six displacement (D) sensors attached to section A-A to observe the girder deflection and twelve strain (S) sensors are used to monitor the slab and girders stresses. Sensors S7 and S8 are utilized to measure the slab strain, sensors S1 to S6 are used to measure the girders bottom flanges stresses, sensors S9 and S10 are used to observe the girders G1 and G2 top flanges stresses, and sensors S11 and S12 are used to measure the stresses of the G1 and G2girders' webs, as presented in Fig. 2(a). As presented in Figs. 1 and 2, the distribution of the sensors is used mainly to measure the slab deflection. Thirteen displacement sensors are used to measure the slab deflection, four strain sensors are used to measure the stress of the slab and three accelerometers are utilized to observe the slab vibration. The strain sensors are supported on a steel plate attached to the bridge slab, as presented in Fig. 2(c).

**Table 1 Monitoring system contents and properties**

Equipment name	Model (standard)	Usage	Remarks
Digital Strain Meter	TC-32k	Check sensors abnormality	Japan, TML Inc.
Data Logger	DS-NET	Record the static and dynamic data	Austria, DS-NET Inc.
Software	DIADEM	Data analysis, storage, display	USA, NI Inc.
Strain Gauge	PL-60-11-1L	Strain measurements (for concrete)	Japan, TML Inc.
	WFLA-6-11-1L	Strain measurements (for steel)	Japan, TML Inc.
Accelerometer	ARF-10A	Acceleration measurements	Japan, TML Inc.
Displacement Meter	CDP-50	Deflection measurements	Japan, TML Inc.



**Fig. 3 Truck dimensions and axle (units in mm)**

**Table 2 Static loading cases of PSC girder and RC slab**

Section	Loading case	Truck direction	Lane	Lane direction
PSC Girder	L.C 1	A2 → A1	2	Mullae-dong
	L.C 2	A2 → A1	1	Mullae-dong
	L.C 3	A2 → A1	Center line	Mullae-dong
	L.C 4	A2 → A1	Center line	Dorim-dong
	L.C 5	A2 → A1	1	Dorim-dong
	L.C 6	A2 → A1	2	Dorim-dong
RC-Slab	L.C 1	A2 → A1	2	Mullae-dong
	L.C 2	A2 → A1	1	Mullae-dong
	L.C 3	A2 → A1	1	Dorim-dong
	L.C 4	A2 → A1	2	Dorim-dong

*2.2 Loading cases*

The testing vehicle, shown in Fig. 3, has been designed to deliver the ultimate live loads specified by the AASHTO Code. The vehicle is a 3-axle dump truck fully loaded with sand, weighing, in excess of 26 tons when fully loaded, that are distributed as follows: A=5.44 tons and B=20.56 tons (see Fig. 3). The time lag between tests conducted for each phase did not allow for the sand to be kept in the dump trucks. An effort was made to have consistent loads for the static and dynamic test phases.

In the static test, six loading cases (LC 1~6) are conducted for the PSC girder and four (LC 1~4) for RC slab, as shown in Table 2 and Fig. 4. In Table 2, the direction A2 to A1 refers to the direction to Mullae-dong, and via versa for the A1 to A2. Fig. 4(a) illustrates the static loading cases of LC1 and LC2 for the PSC girder, in this

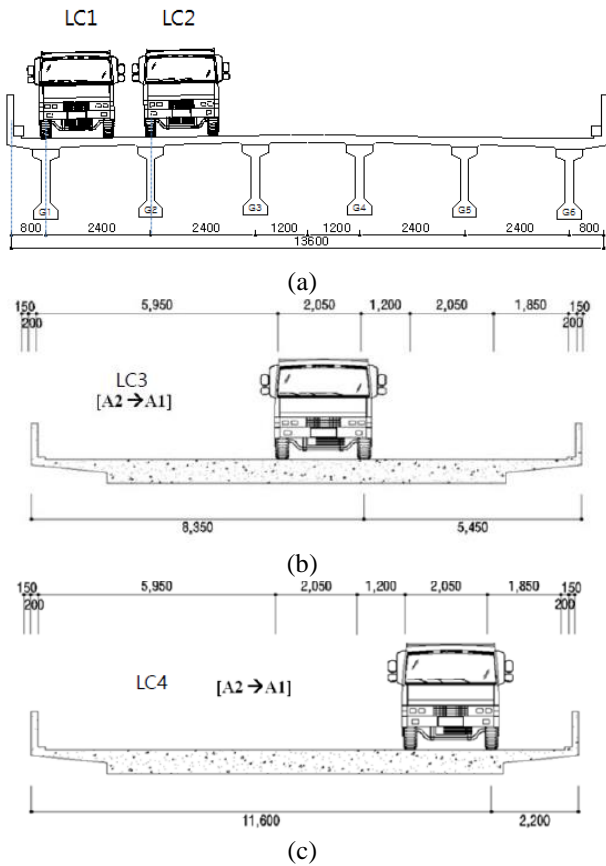


Fig. 4 Static test for the (a) PSC girder and (b and c) RC slab of the bridge

Table 3 Dynamic cases of PSC girder and RC slab

Section	Load case	Truck Direction	Lane	Speed	Lane direction
PSC Girder RC-Slab	L.C 1	A2 → A1	1	10 km/h	Mullae-dong
		A1 → A2	1	10 km/h	Dorim-dong
	L.C 2	A2 → A1	1	20 km/h	Mullae-dong
		A1 → A2	1	20 km/h	Dorim-dong
	L.C 3	A2 → A1	1	30 km/h	Mullae-dong
		A1 → A2	1	30 km/h	Dorim-dong
L.C 4	A2 → A1	1	40 km/h	Mullae-dong	
	A1 → A2	1	40 km/h	Dorim-dong	
L.C 5	A2 → A1	1	50 km/h	Mullae-dong	
L.C 6	A2 → A1	1	60 km/h	Mullae-dong	

case, the wheel position of trucks was designed to concentrate the loads on the girders, as shown in Fig. 4(a) for load cases 1 and 2. In addition, Fig. 4(b) and (c) demonstrate the static loading cases and the positions of trucks for the RC slab tests of LC3 and LC4. This test is used to extract the maximum behavior of the bridge girder and slab and check the neutral axis of the PSC beam girder.

In this case, the truck is moved on the bridge to record the maximum observed strain and then the truck return back

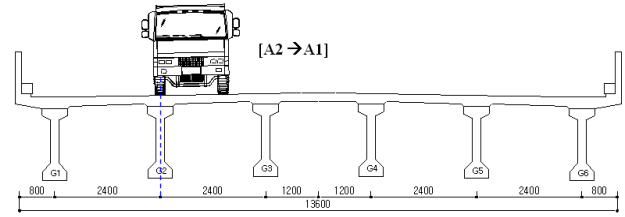


Fig. 5 LC1~6 dynamic load test of the PSC bridge girder

to stay over for ten minutes above the point that recorded the maximum strain value. The data of the sensors are filtered and evaluated to record the maximum strain and deflection values. For the RC slab, the static loads are conducted at spans S16, S17 and S18 to measure the maximum and minimum tensile and compressive strains of the bridge deck, as well as, to measure the maximum and minimum deflection responses of the bridge deck.

Different truck speeds from 10 to 60 km/h are used to assess the semi-static and dynamic behaviors of the bridge girder and slab. Table 3 shows the dynamic loading cases of the girder and slab of the bridge. It is noted that speeds lower than 80 Km/h have less effects on bridges' dynamic responses (Grubb *et al.* 2007, Mohseni *et al.* 2018). However, vehicle speed is among other factors affecting the dynamic behavior of concrete bridges such as bridge span and road surface condition (Deng *et al.* 2011).

In addition, Deng and Cai (2010) concluded that variety of vehicle speeds should be considered when testing the dynamic behavior of bridges to reflect the bridges' real performance. ISO (1995) considered vehicle speeds from 30-120 km/h to cover the whole conditions of bridges. Furthermore, Issa and Shahawy (2004), Kim *et al.* (2008), Nguyen and Tran (2015) and Gunter (2016) utilized 10-100 Km/h vehicle speeds to evaluate the dynamic and semi-static performances of prestressed girders of different types of bridges. The current study has covered a real range of forces produced by applying the selection speeds on the bridge girder and slab. Fig. 5 illustrates the position of the test truck over the bridge. In the current study, a constant distance between the trucks and the bridge handrail of lane 1 by 3,200 mm, as presented in Fig. 5. The dynamic loads depends on many parameters that are studied separately in the design stage, these parameters include the span length, truck weight, axle loads, axle configuration, position of the vehicle on the bridge, number of vehicles on the bridge, girder spacing, and stiffness of structural members (slab and girders) (Nowak and Szerszen 2000). The monitoring system is used to find out the overall bridge performance considering all the above parameters. In addition, the same conditions for the vehicles' speeds and positions of the previous tests are considered in this study.

### 2.3 Dynamic evaluation methods

To assess the dynamic behavior of structures in time domain, the semi-static and dynamic performances of structures should be separated and classified. In this study, the wavelet denoise method is used to extract the semi-static performance components of bridge girder and slab. It is reported that the wavelet denoise method is efficiently

used to remove the dynamic and sensors noises (Kaloop *et al.* 2017). Herein, the strain and displacement observations comprise the maximum dynamic responses, while the smoothed measurements contain the maximum semi-static response of structures. However, to investigate the effect of moving trucks over the bridge, the dynamic amplification factors (DF) is defined as (Huang 2001)

$$DF(\%) = \left[ \frac{R_d}{R_s} - 1 \right] * 100 \quad (1)$$

where  $R_d$  and  $R_s$  are the dynamic and semi-static responses, respectively, of strain or displacement measurements. The DF can be used to assess truck speeds effect and moving directions, as well as to study the bridge load capacity and evaluate the safety of the bridge girder and slab.

Reliability is the most important factor when studying the serviceability and safety of structures in time domain (Modares and Taha 2014). The common method used to study the reliability of structures is the probabilistic evaluation of the performance measurements (Modares and Taha 2014, Strauss *et al.* 2009, Ren and Yue 2018). Many static methods including probabilistic can be used to evaluate a real time measurements (Nowak and Szerszen 2000, Strauss *et al.* 2009). Although, the normal distribution is usually used to assess the response of SHM data, it is not appropriate for survival analysis, like bridges evaluation, because, survival data are usually censored and incomplete, and the shape of the survival time distribution is skewed (Nabizadehdarabi 2015). Therefore, distributions such as exponential, Weibull, lognormal, gamma, Gompertz, and log logistic are typically considered for survival analyses (Nabizadehdarabi 2015). Sobanjo (2011) found that the Weibull distribution is suited to the times data, and Leira *et al.* (2017) concluded that it gives a good correlation with the time data measurements. Therefore, the Weibull distribution is used to assess the reliability of Dorim-Goh bridge. The Weibull is a statistical method that uses the probability distribution parameters to describe the relationship between accumulated failure time and test time (Verma *et al.* 2016). This approach is applied to study the effect of loads on structures' reliability (Verma *et al.* 2016, Kaloop *et al.* 2017, Hill and Okoroafor 1995). The strain measurements are used to assess the bridge reliability, while the dynamic effect of strain measurements is shown high impact than it for the displacement measurements, as will be presented latter. The Weibull distribution for strain measurements is given by (Dinler and Akdag 2009)

$$f(s) = k/c \left( \frac{s}{c} \right)^{k-1} e^{-\left( \frac{s}{c} \right)^k} \quad (2)$$

where,  $f(s)$  is the probability of measuring strain  $s$ ,  $k$  dimensionless shape parameter and  $c$  is the scale parameter in strain units. The scale parameter represents the measurements distributions. The shape parameter is utilized to observe the reliability of structures (Verma *et al.* 2016), this parameter describes failure state during testing and depends on whether the  $k$  value increases/decreases or remains constant over time (Verma *et al.* 2016). The reliability is decreasing or increasing over the monitoring

time, when the  $k$  is greater or lesser than one, respectively. However, the bridge behavior remains constant over the testing time when  $k$  equals one (Verma *et al.* 2016, Hill and Okoroafor 1995). A graphical method, designed using the cumulative distribution function (CDF) of weibull distribution (Dinler and Akdag 2009, Seguro and Lambert 2000), is used to calculate these parameters, as follows

$$F(s) = 1 - e^{-\left( \frac{s}{c} \right)^k} \quad (3)$$

Twice logarithm of CDF, Eq. (3), is taken to obtain the weibull parameters, as follows

$$\ln[-\ln[1 - F(s)]] = k \ln s - k \ln c \quad (4)$$

The pairs of  $(\ln s, \ln[-\ln[1 - F(s)]])$  are used to obtain the linear equation parameters  $y = ax + b$  which considered the relation between the two pairs. Hence, the least square method is used to estimate the Weibull parameters from linear equation, and they can be calculated as follows:  $k = a$ , and  $c = \exp(-b/a)$ .

In the other hand, to evaluate the bridge behavior in frequency domain, the wavelet analysis is used with the acceleration measurements. The wavelet energy and first domain frequency parameters are evaluated and assessed. The fast Fourier transformation (FFT) is used to estimate the frequency contents of signals and the results are compared with the results of a finite element model. The wavelet decomposition is used to extract the wavelet energy (Sayed *et al.* 2017). The acceleration signals are divided into approximate (a) "passing through high-pass filter" and details (d) "passing through low-pass filter" components. The decomposition of the original signal ( $S$ ) at each decomposition level ( $i$ ) can be represented as follows

$$S_i(t) = a_{i+1}(t) + d_{i+1}(t) \quad (5)$$

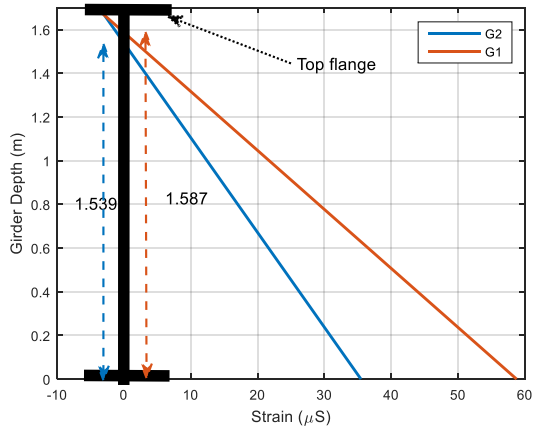
The number of decomposition levels of the signal can be computed based on the sensor sampling frequency and structures FEM frequency calculations (Sayed *et al.* 2017), and that divided the signals based on the time interval ( $\Delta t$ ). For the acceleration signals, the details components only can be used to reconstruct the original signal without dynamic information losses of the structures (Sayed *et al.* 2017). Therefore, the original signal can be expressed as follows

$$S(t) = \sum_{j=1}^n d_j(t) \quad (6)$$

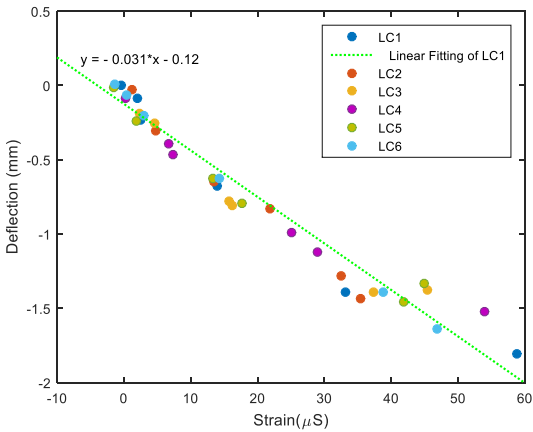
where,  $n$  is the total number of decomposition levels. Herein, the Daubechies wavelet basis function is used to extract the detailed acceleration measurements components, presented as

$$d_j(t) = \sum_{m=-\infty}^{\infty} C_{j,m} \varphi_{j,m} \quad (7)$$

where,  $m$  indicates an index of time scale,  $C_{j,m}$  are the wavelet coefficients, and  $\varphi_{j,m}$  are the basis functions. Therefore, the wavelet energy can be calculated at each level using the detailed components for that level. The wavelet energy ( $E$ ) can be expressed as follows



(a)



(b)

Fig. 6(a) strain distribution along bridge girder, (b) bottom strain-deflection relationship of girder

$$E = \Delta t \sum_{j=1}^n \sum_{i=0}^t d_j^2(t) \tag{8}$$

Therefore, the frequency components can be represented in time domain to check the bridge frequency performance along the monitoring time.

### 3. Results and discussion

#### 3.1 Static evaluation

The strain and deflection of bridge girder are presented in Fig. 6 and Table 4. The strain distribution along the girders G1 and G2 are shown in Fig. 6(a). The maximum tensile strain at the bottom flanges of girders G1 and G2 are observed under LC1 and LC2, respectively, while the maximum compressive strain of points S7 and S8 are 4.18 and 3.7μs, respectively, under the same loading conditions.

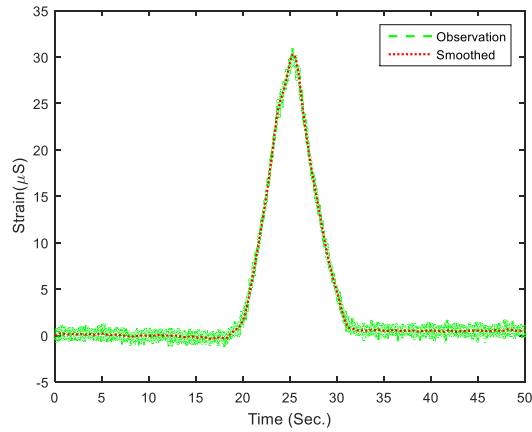
From Fig. 6(a), it can be seen that the neutral axis position at 1.587 and 1.539 m for girders G1 and G2, respectively, and this is compared with the theoretical neutral axis calculation of the bridge girder. As a result, the measured neutral axis position of the girders is deviated within 5% from the theoretical neutral axis position, and

Table 4 Strain measurements under static load cases for section A-A (units: μs)

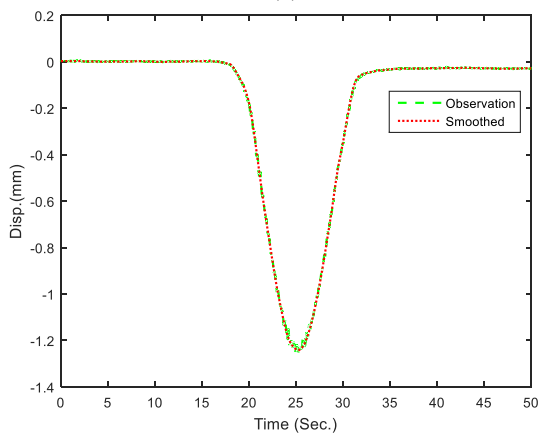
Sensor	LC 1	LC 2	LC 3	LC 4	LC 5	LC 6
S7	-4.18	-2.76	4.11	-2.22	-0.75	-0.48
S8	-4.8	-3.7	2.55	-4.38	-2.86	-2.89
S9	-1.29	-3.23	0.61	-3.58	-1.14	-1.09
S10	-3.71	-2.5	1.44	-5.47	-4.09	-2.48
S11	29.13	7.05	0.74	-1.9	-2.39	-0.92
S12	18.49	21.93	10.02	1.24	-1.83	-2.26

Table 5 RC slab response under static loads effects (units: strain(μs), deflection (mm))

Section	Sensor	LC 1			LC 2		
		S18	S17	S16	S18	S17	S16
B-B	D1	0.003	0.000	-0.582	0.002	0.001	-0.293
	D2	0.001	-0.002	-0.399	0.002	0.002	-0.362
	D3	0.001	-0.002	-0.297	0.002	0.000	-0.37
	D4	0.000	-0.001	-0.216	0.003	0.002	-0.337
	D5	0.001	0.000	-0.095	0.002	0.002	-0.239
C-C	S1	0.40	-23.46	-0.02	0.68	-5.98	1.18
	S2	0.68	-9.99	0.27	0.44	-10.16	0.94
	S3	0.53	-3.68	0.38	0.72	-7.62	1.05
	S4	0.30	0.08	0.89	1.80	-3.24	1.29
	D6	0.013	-0.224	-0.003	0.019	-0.079	0.000
	D7	0.023	-0.19	-0.01	0.027	-0.193	-0.007
	D8	0.027	-0.122	-0.002	0.028	-0.227	-0.003
	D9	0.022	-0.054	-0.002	0.024	-0.159	-0.004
	D10	0.007	0.002	0.004	0.008	-0.038	-0.012
	D11	-0.646	0.008	-0.003	-0.363	0.023	0.002
D-D	D12	-0.522	0.023	-0.005	-0.46	0.027	0.001
	D13	-0.356	0.014	-0.014	-0.484	0.024	-0.002
Section	Sensor	LC 3			LC 4		
		S18	S17	S16	S18	S17	S16
B-B	D1	-0.001	-0.004	-0.242	-0.001	-0.005	-0.095
	D2	0.000	-0.004	-0.336	-0.001	-0.005	-0.209
	D3	-0.002	-0.006	-0.379	-0.001	-0.004	-0.292
	D4	-0.002	-0.005	-0.383	-0.001	-0.006	-0.397
	D5	-0.001	-0.005	-0.31	0.001	-0.005	-0.583
C-C	S1	2.17	-2.96	0.58	1.49	0.21	0.82
	S2	1.32	-9.21	0.86	1.25	-2.84	1.58
	S3	0.52	-9.92	0.82	1.29	-8.34	1.39
	S4	0.77	-7.84	-0.04	1.38	-22.06	1.12
	D6	0.011	-0.059	-0.007	0.011	-0.005	-0.001
	D7	0.012	-0.164	-0.02	0.021	-0.051	-0.01
	D8	0.026	-0.227	-0.008	0.027	-0.124	-0.007
	D9	0.016	-0.192	-0.013	0.023	-0.174	-0.005
	D10	0.011	-0.034	-0.012	0.006	-0.172	-0.017
	D11	-0.294	0.021	-0.003	-0.1	0.012	-0.009
D-D	D12	-0.402	0.024	-0.002	-0.195	0.02	-0.006
	D13	-0.480	0.023	-0.005	-0.316	0.018	-0.007



(a)



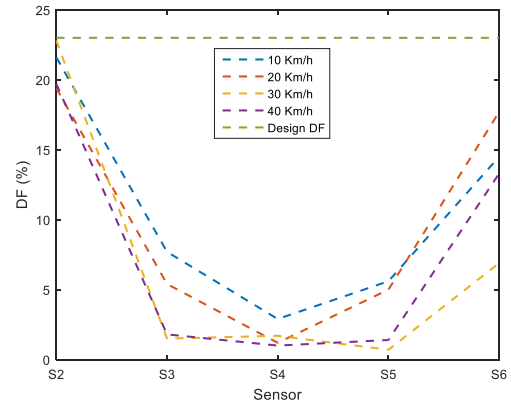
(b)

Fig. 7 Bridge girder performance under 10 Km/h, (a) S2 strain, (b) D2 displacement

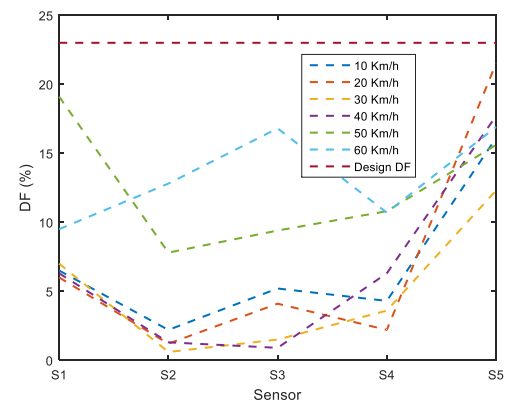
this means that there is no abnormal behavior occurred. The relationship between the strain and deflection of the bridge girders is shown in Fig. 6(b). A linear correlation between the two responses is observed. The maximum strain and deflection are observed at girder G1 under loading case LC1. In addition, the linear fitting of the relationship between strain and deflection for the LC1 is presented in Fig. 6(b).

The correlation coefficient (R2) of linear fitting of strain and deflection of the bridge girder is 0.96, it means that the performance of the bridge is controlled and the bridge girder behavior is safe under static loads. The strain observation of the slab and the girder top flange and web under the six loading cases are shown in Table 4. It is noted that the maximum tensile strain occurs with LC1 ( $29.13\mu s$ ), while the maximum compressive strain is observed with LC4 ( $-5.47\mu s$ ). In conclusion, the strain and deflections observed values for the static test shows that the bridge behavior is safe based on the calculation and AASHTO rules, within 5% from the neutral axis (Wassef *et al.* 2003).

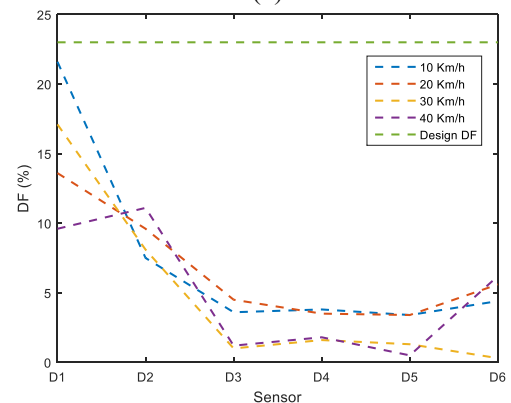
The strain and deflection observations for the RC slab are presented in Table 5. The maximum tensile strain occurs at section C-C ( $2.17\mu s$ ) with loading case LC3 on span S18, while the maximum compressive strain is  $22.06\mu s$  under LC4 on span S17. The deflection measurements show that the maximum deflection of section B-B is 0.583 mm and



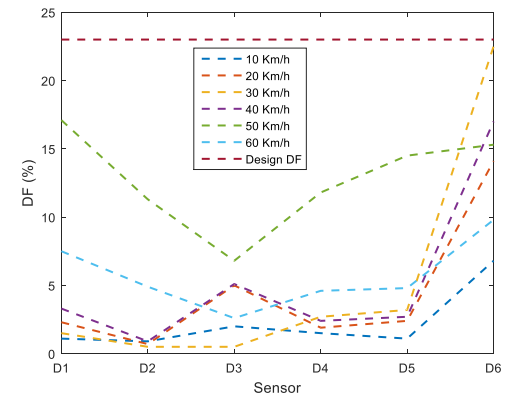
(a)



(b)



(c)



(d)

Fig. 8 DF of bridge girder for (a) strain of A1-A2 direction, (b) strain A2-A1 direction, (c) displacement A1-A2 direction and (d) displacement A2-A1 direction

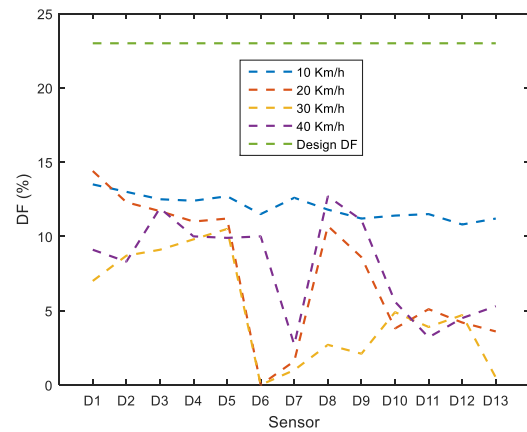
this occurred with loading case LC4 when the load over S16. In addition, the maximum deflection is 0.227 mm at section C-C that observed with LC3 over the span S17, while the maximum deflection of section D-D is 0.646 mm, with LC1 over the span S18. In addition, the range of changes of strain and deflection are small, as seen in Table 5. Moreover, the deflection measurements show that the symmetry of deflection by loading test truck on each lane is approximately same at each section for the different cases of loads. This indicates that there is no specific changed in the structure behavior, while the maximum deflection of the bridge slab is 80.302 mm based on finite element model analysis.

### 3.2 Dynamic evaluation

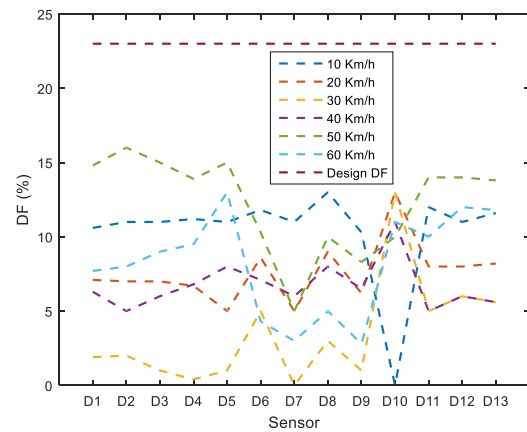
To evaluate the bridge safety, the DF, reliability and dominant frequency of the bridge girders and deck are assessed. The strain and displacement data collected are filtered to extract the semi-static performances for both measurements. Fig. 7 shows the observed and filtered data of the bridge girder under truck speed 10 Km/h to Mullae-dong. The low-pass filter is used to filter the measurements. As shown in Fig. 7, the low-pass filter can be used to extract the semi-static strain and displacement measurements, and these extraction performances can be used to calculate the DF of the bridge girder.

Fig. 8 shows the DF of the bridge girder for the strain and displacement measurements. In addition, Fig. 9 demonstrates the DF of the bridge slab sections. The parameters affected the DF calculations are the truck speed and position. From Fig. 8, the DF values for the bridge girder and slab are lower than the DF design value, it means that the bridge dynamic behavior is safe. The maximum DF value is observed at points close to the truck pass. For example, the maximum DF of the bridge girder is located at girders G1 and G2, as presented in Figs. 8(a) and (c), when the truck passing from A1 to A2. Meanwhile, the maximum DF values are extracted at girders G5 and G6, as shown in Figs. 8(b) and (d). In contrast, the variations of DF values are high in bridge slab performance. As presented in Figs. 9(a) and (b), the truck position does not affect the DF values. In the other hand, the truck speed affects more the DF values of the bridge. For instance, the 10 Km/h speed has the highest effect than other speeds in the direction A1 to A2, while the speed 50 Km/h has the highest effect than other speeds in the direction A2 to A1 for the bridge girder and slab. Moreover, the correlation between the DF values of the bridge girder under different speeds is higher than that with the bridge slab. Also, the correlation of the DF values of the bridge girder for the direction A1 to A2 is higher than that observed in the direction A2 to A1. In addition, from Figs. 8 and 9, the correlation between DF of the bridge slab is lower than that for the bridge girder, which implies that the section stiffness affects the DF values. Furthermore, the DF values for the bridge girders are affected by the bridge torsion as presented in Figs. 8(a), since the DF values for the S2 and S6 are higher than the S3, S4 and S5.

These results reveal that the DF values can be used to assess the bridge safety considering traffic speeds effects.



(a)



(b)

Fig. 9 Displacement DF of bridge slab for (a) A1-A2 direction, (b) A2-A1 direction

Low speed affects more the DF values, and this may be due to the longer time period the truck took from entering the monitored span till leaving it. Moreover, the sensitivity of the bridge slab sections for the affected loads is higher than that observed on the bridge girder due to the section stiffness. The torsion of the bridge girders is higher than that occurred on the bridge slab under different speeds.

In term of reliability analysis, the strain measurements of the S2 points of the bridge girder and slab are selected to assess the serviceability of the bridge with different speeds. Fig. 10 illustrates the graphical method performance to detect the Weibull parameters for the strain measurements of the bridge girder with 60 Km/h. The least square method is used to estimate the linear fitting parameters, weibull parameters, for the linearized strain data. The autocorrelation between linearized and linear fitting is 0.93.

In addition, the CDF calculations using the weibull method and strain measurements are presented in Fig. 10(b). The autocorrelation coefficients between the CDF of the strain measurements and Weibull cumulative probability density function (WCDF) is 0.96. These results show that the hypothesis testing for the bridge performance with weibull method is good and the estimated weibull parameters can be used to assess the bridge behavior.

Fig. 11 illustrates the CDF of the strain measurements of the bridge girder and slab with truck speeds in A1-A2

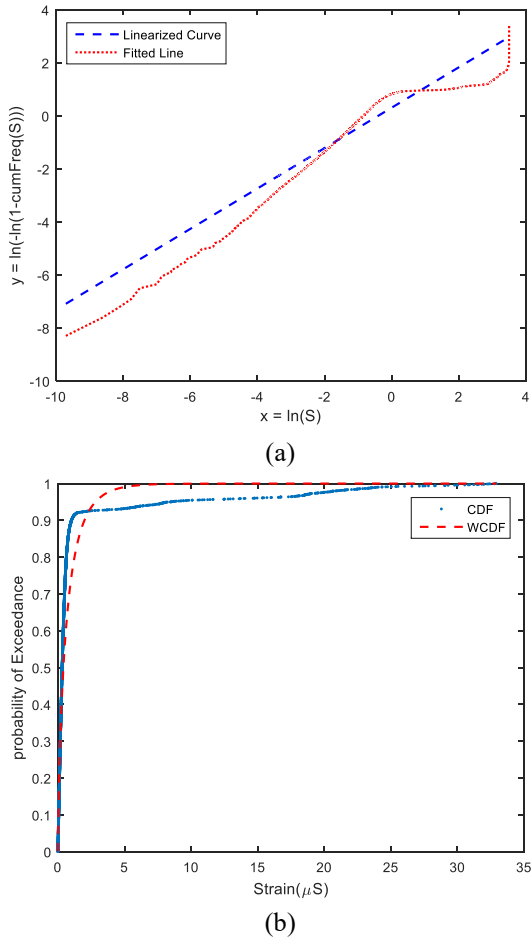


Fig. 10 Weibull parameters evaluation (a) graphical method and (b) CDF performances

direction. Table 6 concludes the Weibull probability parameters with different truck speeds. The strain measurements probability are affected by the truck speeds, as seen in Fig. 11, while the probability increased with increasing the truck speeds.

In addition, the strain measurements probability of the bridge slab has higher correlation than that of the bridge girder with different loads. Therefore, the reliability of the bridge girder and slab is affected by the traffic speeds, in addition, the sensitivity of the bridge girder is higher than the bridge slab for different truck speeds. From Table 6, it can be seen that the variation of weibull scale parameters is high which means that the strain measurements distribution is affected by the truck speeds. While, the distribution change of the bridge slab is approximately similar after truck speed of 30 km/h. Meanwhile, the weibull shape parameters that presented in Table 6 show that the failure rate of the bridge girder and slab is decreased. The weibull shape parameters for the speeds 20, 30 and 40 Km/h in direction A2 to A1 are approximately equal one for the bridge girder and slab, it means that the failure rate is constant. Also, in the direction A1 to A2, the weibull shape parameters for the speeds 50 and 60 Km/h are close to one. Consequently, the traffic direction and high speed affect the failure rate of the bridge slab and girder. From these results, the reliability of bridge is safe with the existing conditions.

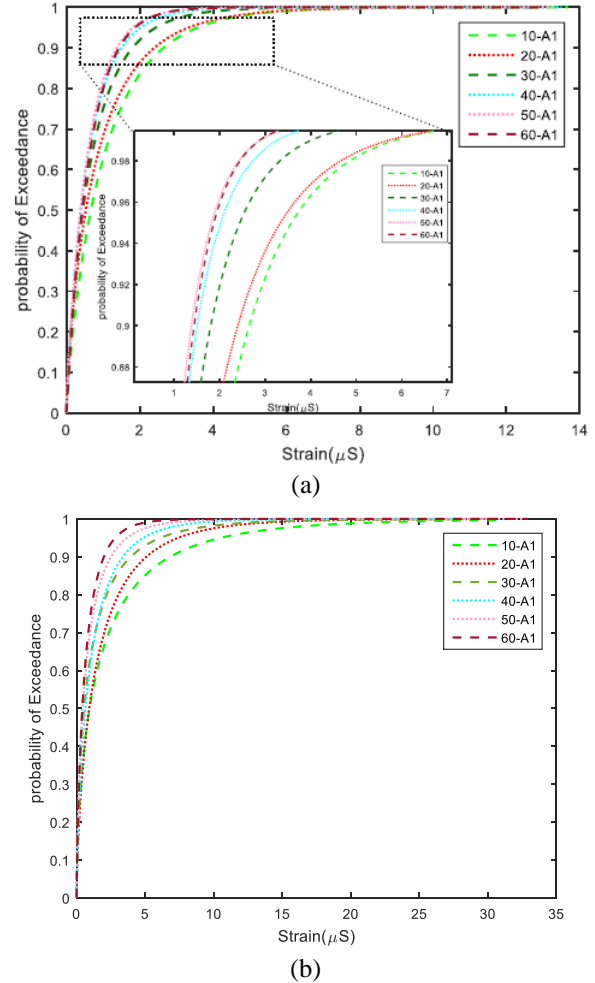


Fig. 11 Weibull CDF of strain measurements of (a) bridge slab and (b) bridge girder

Table 6 Weibull probability parameters of bridge slab and girder

Speed & Direction	Slab		Girder	
	K	C (μs)	K	C (μs)
10 Km/h - A1 to A2	0.873	1.018	0.608	1.731
10 Km/h - A2 to A1	0.897	0.788	0.872	0.829
20 Km/h - A1 to A2	0.797	0.842	0.700	1.545
20 Km/h - A2 to A1	0.909	0.847	0.980	0.814
30 Km/h - A1 to A2	0.866	0.688	0.604	0.990
30 Km/h - A2 to A1	0.955	0.586	0.983	0.730
40 Km/h - A1 to A2	0.895	0.593	0.719	1.057
40 Km/h - A2 to A1	0.995	0.568	0.963	0.604
50 Km/h - A1 to A2	0.941	0.568	0.687	0.743
60 Km/h - A1 to A2	0.999	0.624	0.762	0.666

Based on the DF evaluation, the bridge performance under 10 Km/h is selected to present the frequency and reliability performance of the bridge girder and deck. The wavelet details of levels one to six for the acceleration ACC2 of girder and ACC1 of slab for the direction A1 to A2 are presented in Fig. 12. The vibration performance is

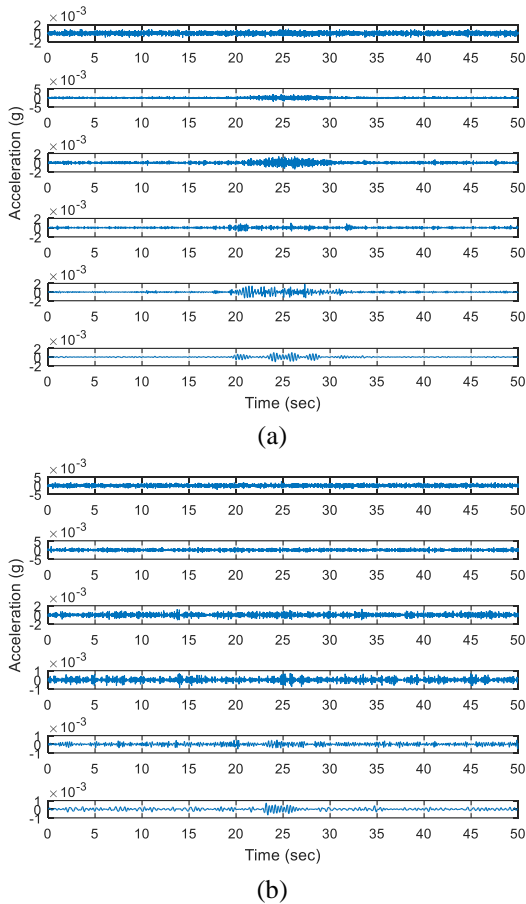


Fig. 12 Wavelet detail contents of (a) ACC2 of girder and (b) ACC1 of slab

clearly shown in the bridge girder at level 2, while the vibration performance for the bridge slab appears at level three. Because of the section stiffness, the dynamic noise of bridge slab is high.

The wavelet energy of each level is calculated and presented in Fig. 13. As shown, the bridge girder wavelet energy is affected when the truck passes over the monitored point. It is observed that the levels one, two and five are common due to dynamic effect of moving truck. In the other side, the bridge slab wavelet energy has less effect due to truck passing over the monitored section. Moreover, the energy of the signal contents decreases with the wavelet number. Therefore, to reconstruct the signals for the bridge girder and slab, the effective wavelet levels are selected. In this case, the levels one, two and five are selected to reconstruct the bridge girder signals, while the whole details levels are used to rebuild the bridge slab signals. The reconstructed data are used to define the dominant frequencies of the bridge girder and slab. The first mode of the bridge frequencies of girder (ACC2) and slab (ACC1) are calculated and presented in Figs. 14(a) and (b), respectively, for the bridge performance under 10 Km/h in direction A1 to A2. In addition, Fig. 14(c) summarizes the first mode frequencies calculation of the bridge girder (G) and slab (S) monitored points under different truck speeds.

From Fig. 14, the reconstruction signals can be used to extract the frequencies contents of the bridge under

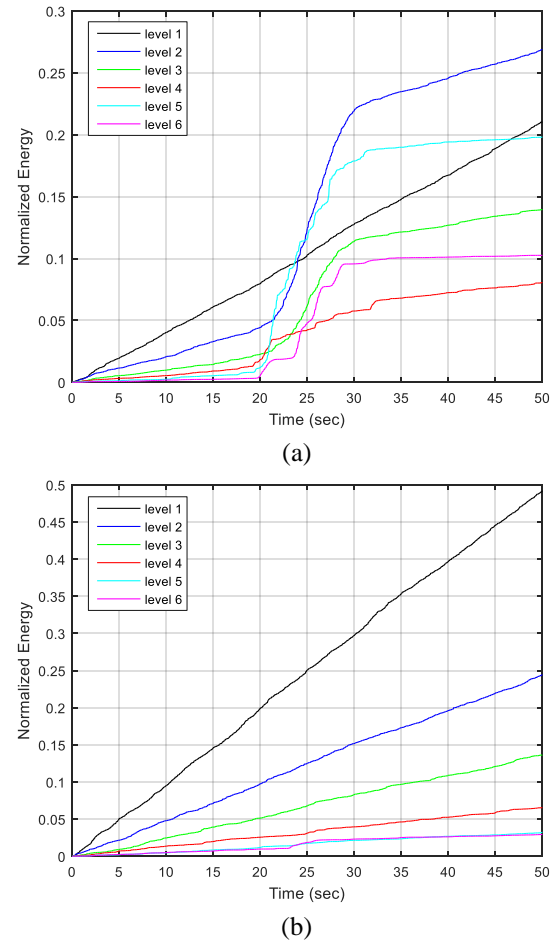
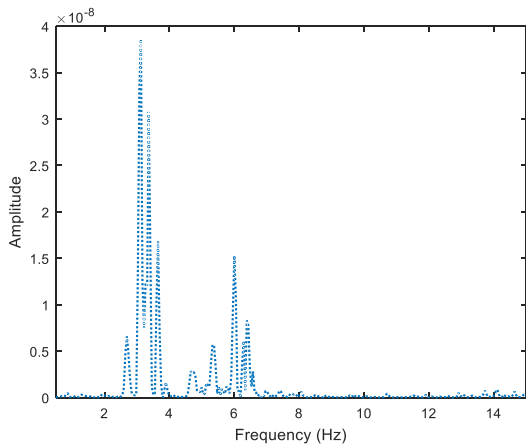


Fig. 13 Wavelet energy of (a) ACC2 of girder and (b) ACC1 of slab

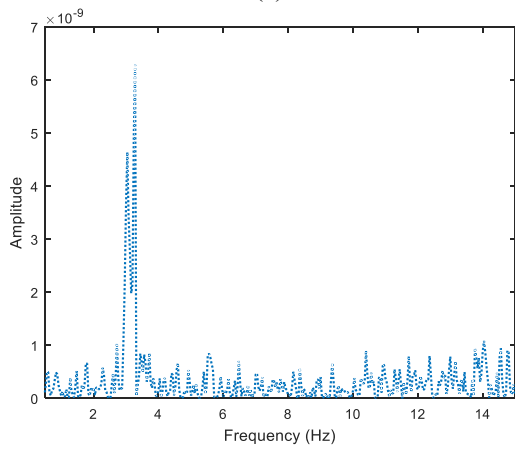
different loads effects. The first modes of the slab sections are highly correlated and the values are the same with each case. This indicates that the bridge slab is safe in frequency domain with different load cases. Moreover, the first mode of the bridge slab is higher than the design value based on the simulation model of the bridge (2.3 Hz). Moreover, the first mode of the bridge girder frequency G2 is different some time relating to the slab of the same section. The maximum change between frequencies of the two girder points is 0.1 Hz, but the two points' frequencies are higher than the simulation model calculation by 25% in average. It means that the vibration behavior of the bridge is lower than the design performance of the bridge. Therefore, the bridge girder is also safe in frequency domain with different truck speeds.

#### 4. Conclusions

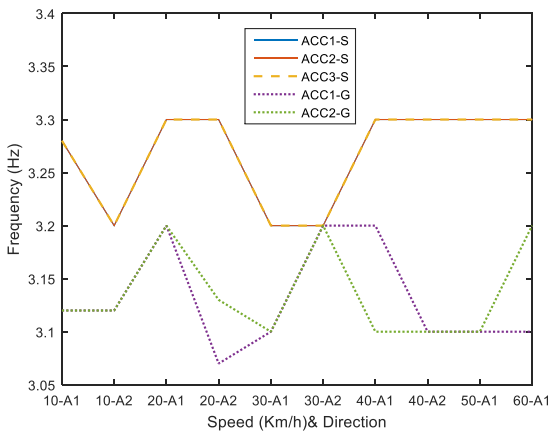
To study the full behavior of Dorim-Goh bridge, static and dynamic tests are conducted using short period monitoring system. The strain, displacement and acceleration measurements are collected to evaluate the performance of the bridge girder and slab. The distribution of strain along the bridge girder is studied and linear fitting are used to assess the static behavior measurements. The



(a)



(b)



(c)

Fig. 14 Frequency contents of (a) ACC2 of girder, (b) ACC1 of slab and (c) conclusion the dominant frequencies calculation

dynamic amplification factor and reliability are assessed to evaluate the bridge safety. In addition, the wavelet analysis is used to filter the measured data and evaluate the bridge behavior in frequency domain. The results of the bridge performance with different loading cases show that the bridge is safe in time and frequency domains, and the major conclusions of this study are as follows:

- The measured neutral axis position of the girders is deviated within 5% from the theoretical neutral axis

position, and this means that there is no abnormal behavior occurs, in addition, the symmetry of deflection by the test truck on each lane is approximately the same and this indicates that there is no specific structural behavior change under static loads.

- The DF values for the bridge girder and slab are lower than the DF design value, it means that the bridge dynamic behavior is safe. The truck speeds and bridge torsion affect the DF values. Moreover, the sensitivity of bridge slab sections for the loads is higher than that observed on the bridge girder due to the section stiffness.

- The shape parameter of Weibull probability method is used to study the reliability of the bridge, the reliability is affected by the traffic direction and truck speeds. In addition, the weibull shape parameters show that the failure rate of the bridge girder and slab are almost decreased, and the bridge reliability is safe with the existing conditions.

- The wavelet energy of vibration performance of the bridge girder occurs mainly over three levels for the bridge girder, while that observed over the whole levels for the bridge slab. These levels are used to reconstruct the acceleration performance of the bridge, and the results show that the frequencies contents are shown clearly. The first mode of the bridge slab and girder are higher than the design value by 25%, it means that the bridge is safe in frequency domain.

### Acknowledgements

This work was supported by a 2018 Incheon National University Research Grant. The authors gratefully acknowledge these supports. The authors greatly appreciate Mr. Kyoung Ho Kim's support and help.

### References

Caglayan, B.O., Ozakgul, K. and Tezer, O. (2012), "Assessment of a concrete arch bridge using static and dynamic load tests", *Struct. Eng. Mech.*, **41**(1), 83-94.

Deng, L., Cai, C. and Barbato, M. (2011), "Reliability-based dynamic load allowance for capacity rating of prestressed concrete girder bridges", *J. Brid. Eng.*, **16**(6), 872-880.

Deng, L. and Cai, C. (2010), "Development of dynamic impact factor for performance evaluation of existing multi-girder concrete bridges", *Eng. Struct.*, **32**(1), 21-31.

Dinler, A. and Akdag, S.A. (2009), "A new method to estimate Weibull parameters for wind energy applications", *Energy Convers. Manage.*, **50**(7), 1761-1766.

Ducruet, C., Carvalho, L. and Roussin, S. (2012), *The Flight of Icarus? Incheon's Transformation from Port Gateway to Global City*, Cities, Regions, and Flows, Routledge, 149-169.

Fan, X.P. and Liu, Y.F. (2018), "Time-variant reliability prediction of bridge system based on BDGCM and SHM data", *Struct. Contr. Health Monit.*, **25**(7), e2185.

Fatemi, S.J., Sheikh, A.H. and Ali, M.S. (2018), "Determination of load distribution factors of steel-concrete composite box and I-girder bridges using 3D finite element analysis", *Austr. J. Struct. Eng.*, **19**(2), 131-145.

Farzampour, A., Kamali-Asl, A. and Hu, J. (2018a), "Unsupervised identification of arbitrarily-damped structures using time-scale independent component analysis: Part I", *J.*

- Mech. Sci. Technol.*, **32**(2), 567-577.
- Farzampour, A., Kamali-Asl, A. and Hu, J. (2018b), "Unsupervised identification of arbitrarily-damped structures using time-scale independent component analysis: Part II", *J. Mech. Sci. Technol.*, **32**(9), 4413-4422.
- Grubb, M.A., Corven, J.A., Wilson, K.E., Bouscher, J.W. and Volle, L.E. (2007), *Load and Resistance Factor Design LRFD for Highway Bridge Superstructures-Design Manual*, FHWA NHI07-035, Federal Highway Administration, Washington, D.C., U.S.A.
- Gunter, R. (2016), "Structural evaluation of SCDOT prestressed channel bridges", M.Sc. Dissertation, Clemson University, U.S.A.
- Hill, R. and Okoroafor, E.U. (1995), "Weibull statistics of fiber bundle failure using mechanical and acoustic emission testing: The influence of interfiber friction", *Compos.*, **26**(10), 699-705.
- Huang, D. (2001), "Dynamic analysis of steel curved box girder bridges", *J. Brid. Eng.*, **6**(6), 506-513.
- Hwang, E. and Nowak, A.S. (1989), "Dynamic analysis of girder bridges", *Transport. Res. Rec.*, **4**(3), 85-92.
- ISO (1995), *Mechanical Vibration-Road Surface Profiles-Reporting of Measured Data*, ISO 8068:1995 (E), Geneva.
- Issa, M.A. and Shahawy, M.A. (2004), "Dynamic and static tests of prestressed concrete girder bridges in Florida", *Proceedings of the IABMAS'04 Bridge Maintenance, Safety, Management and Cost*, Kyoto, Taylor & Francis, London, U.K.
- Kaloop, M., Elbeltagi, E., Hu, J. and Elrefai, A. (2017), "Recent advances of structures monitoring and evaluation using GPS-time series monitoring systems: A review", *ISPRS Int. J. Geo-Infomat.*, **6**(12), 382.
- Kaloop, M., Hu, J. and Elbeltagi, E. (2016), "Evaluation of high-speed railway bridges based on a nondestructive monitoring system", *Appl. Sci.*, **6**(1), 24.
- Kaloop, M.R., Hu, J.W. and Bigdeli, Y. (2017), "The performance of structure-controller coupled systems analysis using probabilistic evaluation and identification model approach", *Shock Vibr.*, **2017**.
- Koto, Y., Konishi, T., Sekiya, H. and Miki, C. (2019), "Monitoring local damage due to fatigue in plate girder bridge", *J. Sound Vibr.*, **438**(6), 238-250.
- Kim, J. and Sitar, N. (2013), "Reliability approach to slope stability analysis with spatially correlated soil properties", *Soils Foundat.*, **53**(1), 1-10.
- Kim, S.H., Ahn, J., Jung, C., Jang, J. and Park, Y. (2014), "Behaviour of steel-box semi-integral abutment bridge considering temperature-earth pressure change", *Int. J. Steel Struct.*, **14**(1), 117-140.
- Kim, J.J., Jin, W.N., Ho, J.K., Jae, H.K., Sung, B.K. and Keun, J.B. (2008), "Overview and applications of precast, prestressed concrete adjacent box-beam bridges in South Korea", *PCI J.*, **53**(4), 83-107.
- Ren, X. and Yue, Q. (2018), "Reliability assessment of reinforced concrete structures based on random damage model", *Struct. Infrastruct. Eng.*, **14**(6), 780-790.
- Leira, B., Thöns, S. and Faber, M. (2017), "System reliability of bridge structure subjected to chloride ingress", *Proceedings of the Joint COST TU1402-COST TU1406-IABSE WCI Workshop*, Zagreb, Croatia.
- Li, H., Yi, T., Gu, M. and Huo, L. (2009), "Evaluation of earthquake-induced structural damages by wavelet transform", *Progr. Nat. Sci.*, **19**(4), 461-470.
- Liu, W., Zhang, H. and Rasmussen, K. (2018), "System reliability-based direct design method for space frames with cold-formed steel hollow sections", *Eng. Struct.*, **166**, 79-92.
- Liu, X., Kuang, Z., Yin, L. and Hu, L. (2017), "Structural reliability analysis based on probability and probability box hybrid model", *Struct. Safety*, **68**, 73-84.
- Modares, R. and Taha, J.M. (2014), "Reliability assessment of structures using interval uncertainty analysis", *Proceedings of the 2nd International Conference on Vulnerability and Risk Analysis and Management (ICVRAM) and the Sixth International Symposium on Uncertainty, Modeling, and Analysis (ISUMA)*, Liverpool, U.K., July.
- Monarrez, M.R.P. (2018), "Weibull stress distribution for static mechanical stress and its stress/strength analysis", *Qual. Reliab. Eng. Int.*, **34**(2), 229-244.
- Mohseni, I., Ashin, A., Choi, W. and Kang, J. (2018), "Development of dynamic impact factor expressions for skewed composite concrete-steel slab-on-girder bridges", *Adv. Mater. Sci. Eng.*, **2018**.
- Nabizadehdarabi, A. (2015), "Reliability of bridge superstructures in Wisconsin", M.Sc. Dissertation, University of Wisconsin-Milwaukee, U.S.A.
- Naser, A.F. and Wang, Z. (2013), "Evaluation of the static and dynamic structural performance of segmental pre-stressed concrete box girder bridge after repairing and strengthening", *Front. Struct. Civil Eng.*, **7**(2), 164-177.
- Nowak, A.S. and Szerszen, M.M. (2000), "Structural reliability as applied to highway bridges", *Prog. Struct. Eng. Mater.*, **2**, 218-224.
- Nguyen, T.X. and Tran, D.V. (2015), "Determination of dynamic impact factor for continuous bridge and cable-stayed bridge due to vehicle braking force with experimental investigation", *Proceedings of the 16th Asia Pacific Vibration Conference*, HUST, Hanoi, Vietnam.
- Paeglite, I. and Paeglitis, A. (2013), "The dynamic amplification factor of the bridges in Latvia", *Proc. Eng.*, **57**, 851-858.
- Peiris, A. and Harik, I. (2016), "Load testing of bridges for load rating", *Proceedings of the 7th International Conference on Sustainable Built Environment*, Kandy, Sri Lanka.
- Phares, B., Lu, P., Wipf, T., Greimann, T. and Seo, J. (2013), "Field validation of a statistical-based bridge damage-detection algorithm", *J. Brid. Eng.*, **18**(11), 1227-1238.
- Sayed, M.A., Kaloop, M., Kim, E. and Kim, D. (2017), "Assessment of acceleration responses of a railway bridge using wavelet analysis", *KSCE J. Civil Eng.*, **21**(5), 1844-1853.
- Seguro, J.V. and Lambert, T.W. (2000), "Modern estimation of the parameters of the weibull wind speed distribution for wind energy analysis", *Wind Eng. Industr. Aerodyn.*, **85**(1), 75-84.
- Seo, J., Phares, B., Lu, P., Wipf, T. and Dahlberg, J. (2013), "Bridge rating protocol using ambient trucks through structural health monitoring system", *Eng. Struct.*, **46**, 569-580.
- Seo, J., Hu, J. and Lee, J. (2016), "Summary review of structural health monitoring applications for highway bridges", *J. Perform. Constr. Facilit.*, **30**(4), 04015072.
- Seo, J., Kilaru, C., Phares, B. and Lu, P. (2017), "Agricultural vehicle load distribution for timber bridges", *J. Brid. Eng.*, **22**(11), 04017085.
- Shahsavari, V. (2017), "Condition assessment of bridge structures using statistical analysis of wavelets", Ph.D. Dissertation, Laval University, Laval, Canada.
- Sohn, H., Farrar, C., Hemez, F., Shunk, D., Stinemates, D., Nadler, B. and Czarnecki, J. (2004), *A Review of Structural Health Monitoring Literature: 1996-2001*, Los Alamos National Laboratory Report, LA-13976-MS.
- Sobanjo, J. (2011), "State transition probabilities in bridge deterioration based on Weibull sojourn times", *Struct. Infrastruct. Eng.*, **7**(10), 747-764.
- Strauss, A., Hoffmann, S., Windener, R. and Bergmeister, K. (2009), "Structural assessment and reliability analysis for existing engineering structures, applications for real structures", *Struct. Infrastruct. Eng.*, **5**(4), 277-286.
- Vaez, S. and Saeid, S. (2018), "Reliability-based optimization of one-bay 2-D steel frame", *KSCE J. Civil Eng.*, **7**(22), 2433-

2440.

- Verma, A. K, Ajit, S. and Karanki, D.R. (2016), *Reliability and Safety Engineering*, Springer S., Springer-Verlag London.
- Wassef, W., Smith, C., Clancy, C. and Smith, M. (2003), *Comprehensive Design Example for Prestressed Concrete (PSC) Girder Superstructure Bridge with Commentary (in US Customary Units)*, Report No.: FHWA NHI-04-043, The Federal Highway Administration, U.S.A.
- Wang, N. (2010), "Reliability-based condition assessment of existing highway bridges", Ph.D. Dissertation, Georgia Institute of Technology, Atlanta, U.S.A.
- Womack, B.K., Halling, M. and Bott, S. (2001), *Static and Dynamic Testing of a Curved, Steel Girder Bridge in Salt Lake City, UTAH*, Report No. UT-00-13, Utah Department of Transportation Research Division, Utah, U.S.A.
- Yang, Y., Wang, X. and Wu, Z. (2016), "Evaluation of the static and dynamic behaviors of long-span suspension bridges with FRP cables", *J. Brid. Eng.*, **21**(12), 06016008.
- Yan, J., Deng, L. and He, W. (2017), "Evaluation of existing prestressed concrete bridges considering the randomness of live load distribution factor due to random vehicle loading position", *Adv. Struct. Eng.*, **20**(5), 737-746.
- Zhang, L., Zhang, J., You, L. and Zhou, S. (2018), "Reliability analysis of structures based on a probability-uncertainty hybrid model", *Qual. Reliab. Eng. Int.*, **35**(1), 263-279.

PL